ISSN 2079-0031 (Print) ISSN 2411-0558 (Online)

UDK 539.3 **DOI: 10.20998/2411-0558.2026.02.04**

Makhmatali USAROV, Dr. Phys.-Math. Sci., Professor
Institute of Mechanics and Seismic Stability of Structures named after M.T.Urazbaev, Uzbekistan Academy of Sciences,
Shukhrat ASKARKHODJAEV, Senior Researcher,
Institute of Mechanics and Seismic Stability of Structures named after M.T.Urazbaev, Uzbekistan Academy of Sciences,
Furqat USANOV, Junior Researcher,
Institute of Mechanics and Seismic Stability of Structures named after M.T.Urazbaev, Uzbekistan Academy of Sciences

TRANSVERSE OSCILLATION OF A PLATE STRUCTURE WITH ALL SIDES FIXED UNDER NORMAL LOADS

This article examines the transverse vibration of a rectangular plate structure, with all sides fixed, under normal loads applied to its surface using bimoment plate theory. The problem was solved using the finite difference method. Numerical results for calculating the normal displacements and stresses are presented. Figs.: 12. Table: 2 Refs.: 17 titles.

Keywords: displacements, stresses, moments, bimoments, bimoment theory, normal load, shear load, equations of motion, boundary conditions, finite difference method.

Introduction. Rectangular plate structures are widely used in various fields of construction and industry. External forces acting on a plate structure can be periodic and varying in frequency. When the frequency of external forces coincides with the eigenfrequency of the plate structure, resonance occurs, which can lead to its failure within a short time. When the frequency of external forces varies, it is important to know not only the frequency of the first tone of free vibrations but also the frequencies of several subsequent overtones, which can also cause resonance. Calculating the strength fluctuations of plate structures under normal loads is one of the most important problems in solid mechanics. Such forces can arise, for example, when plate structures come into contact with other structures or with the soil. Below is an analysis of scientific research on calculating the strength fluctuations of plate structures.

ISSN 2079-0031 (Print) ISSN 2411-0558 (Online)

Dynamic calculations of multilayer (three-layer) plates are based on Kirchhoff's hypotheses or refined theories, such as Timoshenko's theory, where the main unknowns are the displacements of the midsurface of the plate [1] and the isotropic material. These equations are used to derive refined vibration equations. The proposed algorithm allows one to determine the stress-strain state of points in a viscoelastic system.

When constructing a theory, the hypotheses and assumptions used in Kirchhoff-Love shell theory lead to significant shortcomings and errors [2]. In these theories, when deriving the vibration equations, the unknowns are the main components of the displacement of points on the midsurface of the filler; there are usually six of them. If the boundary conditions are formulated accurately, the number of unknowns increases to twelve according to the authors of reference [3]. An n-th-order model [4] has also been developed for calculating the shear strain of a functionally graded multilayer composite plate. Article [5] presents an exact solution in which each term of the series is trigonometric and hyperbolic, and identically satisfies the boundary conditions at all four edges. The solution has three terms, with the first term corresponding to the strip case and the other two terms representing edge effects. The method for obtaining the solution is simple and straightforward. To illustrate the method, numerical values of the deflections are calculated and compared with the results of previous studies.

The problem of a uniformly loaded rectangular plate with elements fixed at all edges was solved by Hencky and, independently, by Bubnov. Bubnov performed accurate calculations for several aspect ratios of the plate, while Hencky performed refined calculations only for the case of a square plate [6].

Hutchinson used the solution presented in [7] and compiled a table of deflections for uniformly loaded rectangular plates. Obtaining numerical values of deflections for a rectangular plate can be difficult. In references [8, 9], a unified series of cosines for rectangular rigidly fixed plates was presented.

R. Singhal et al. [10] conducted experimental studies to obtain the eigenfrequencies of vibrations of rectangular plates with various boundary conditions.

In [11], forced vibrations of a viscoelastic three-layer plate of a certain type and some problems using numerical solutions are presented. Methods,

ISSN 2079-0031 (Print) ISSN 2411-0558 (Online)

algorithms, and software have been developed for obtaining resonant frequencies and analyzing vibrations for a rectangular viscoelastic sandwich plate.

A spectral dynamic stiffness model for plate structures reinforced by beams is proposed in [12]. The theory is general enough to allow plate structures to be subject to any arbitrary boundary conditions, but, importantly, the beam stiffeners can have open or closed cross-sections and can be connected to the plates with or without eccentricity.

References [13 – 15] discuss the development of a theory and method for calculating thick plates. The theory and method were developed to evaluate the stress-strain state of thick plates without simplifying hypotheses within the framework of three-dimensional elasticity theory. In developing the theory, all components of strain and stress arising from the nonlinearity of the law of displacement distribution across the plate thickness were taken into account. The equations of plate motion were constructed in terms of forces, moments, and bimoments. The solution method was based on exact expressions in trigonometric functions.

The studies conducted in [16, 17] are devoted to the numerical solution of the problem of transverse vibrations of a multi-story building within the framework of a solid plate model under seismic impact. A cantilevered anisotropic plate is proposed as a dynamic model of the building. The theory for this plate was developed within the framework of three-dimensional dynamic elasticity theory and takes into account not only structural forces and moments, but also bimoments.

Formulation of the problem. Let a rectangular plate structure, with all sides fixed, be subject to a normal load applied along its face, as shown in Figure 1.

ISSN 2079-0031 (Print) ISSN 2411-0558 (Online)

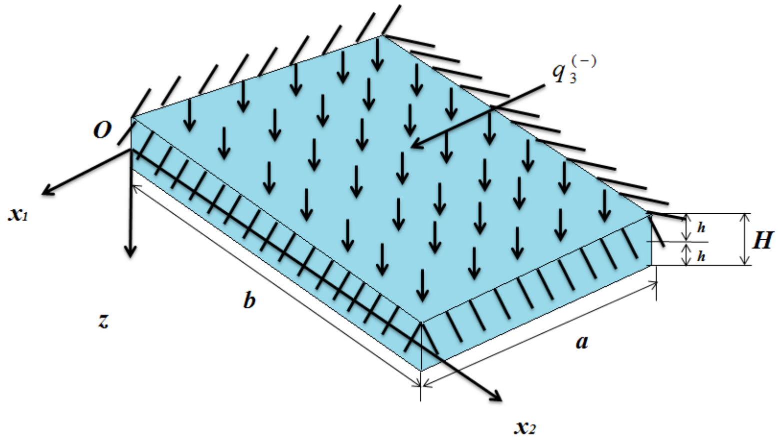

Figure 1. Rectangular plate structure with all sides fixed, subject to normal loads.

We introduce the following notations: plate dimensions in plan a and b, thickness $H = 2h$, where half the thickness of the plate structure is h. To describe the mechanical characteristics of the plate structure, we introduce the following notations: for the elastic moduli E_1, E_2, E_3, for shear moduli G_{12}, G_{13}, G_{23}, for Poisson's ratios: $\nu_{12}, \nu_{13}, \nu_{23}$.

To determine stress through deformation, it is necessary to find the following elastic constants $E_{11},\ E_{12}, ..., E_{33}$, determined through Poisson's ratios and the modulus of elasticity:

$$E_{11} = E_1 g_{11}, \quad E_{22} = E_2 g_{22}, \quad E_{33} = E_3 g_{33},$$
$$E_{12} = E_{21} = E_1 g_{12} = E_2 g_{21}, \quad E_{13} = E_{31} = E_1 g_{13} = E_3 g_{31},$$
$$E_{23} = E_{32} = E_2 g_{23} = E_3 g_{32},$$

ISSN 2079-0031 (Print) ISSN 2411-0558 (Online)

$$g_{11} = \frac{1-\nu_{23}\nu_{32}}{1-\mu^2}, \quad g_{22} = \frac{1-\nu_{13}\nu_{31}}{1-\mu^2}, \quad g_{33} = \frac{1-\nu_{12}\nu_{21}}{1-\mu^2},$$

$$g_{12} = g_{21} = \frac{\nu_{12}+\nu_{13}\nu_{32}}{1-\mu^2} = \frac{\nu_{21}+\nu_{31}\nu_{23}}{1-\mu^2},$$

$$g_{13} = g_{31} = \frac{\nu_{13}+\nu_{21}\nu_{32}}{1-\mu^2} = \frac{\nu_{31}+\nu_{12}\nu_{23}}{1-\mu^2},$$

$$g_{23} = g_{32} = \frac{\nu_{23}+\nu_{13}\nu_{12}}{1-\mu^2} = \frac{\nu_{32}+\nu_{31}\nu_{21}}{1-\mu^2},$$

$$\mu^2 = \nu_{12}\nu_{21}+\nu_{23}\nu_{32}+\nu_{13}\nu_{31}+2\nu_{12}\nu_{23}\nu_{31}.$$

The problem is considered in a rectangular coordinate system. x_1, x_2 and z. Let on the front surface $z=+h$ the plates be subject to external distributed surface normal loads $q_1^{(+)}$, $q_2^{(+)}$, $q_3^{(+)}$ along the corresponding directions of the coordinate axes. Similarly, surface loads are applied to the front surface $q_1^{(-)}$, $q_2^{(-)}$, $q_3^{(-)}$ in the directions of the coordinate axes. In this case, we direct the axis vertically downward along the thickness of the plate structure. The distributed normal surface load is applied to the top face of the plate structure, $z=-h$.

Bimoment theory is based on the well-known Cauchy relations, the generalized Hooke's law, the three-dimensional equations of the general theory of elasticity, and boundary conditions [13 – 15].

Moments, forces, and bimoments are represented by nine unknown functions, listed below:

$$\tilde{W} = \frac{u_3^{(+)}+u_3^{(-)}}{2}, \quad \tilde{r} = \frac{1}{2h}\int_{-h}^{h} u_3 dz, \quad \tilde{\gamma} = \frac{1}{2h^3}\int_{-h}^{h} u_3 z^2 dz,$$
$$\tilde{u}_k = \frac{u_k^{(+)}-u_k^{(-)}}{2}, \quad \tilde{\psi}_k = \frac{1}{2h^2}\int_{-h}^{h} u_k z dz, \quad \tilde{\beta}_k = \frac{1}{2h^4}\int_{-h}^{h} u_k z^3 dz, \quad (k=1,2). \tag{1}$$

Let us write down the equations of motion of the plate with respect to bending, torque moments and relative shear forces [13 – 15]:

ISSN 2079-0031 (Print) ISSN 2411-0558 (Online)

$$\frac{\partial M_{11}}{\partial x_1}+\frac{\partial M_{12}}{\partial x_2}-Q_{13}+H\tilde{q}_1=\frac{H^2}{2}\rho\ddot{\tilde{\psi}}_1,$$
$$\frac{\partial M_{21}}{\partial x_1}+\frac{\partial M_{22}}{\partial x_2}-Q_{23}+H\tilde{q}_2=\frac{H^2}{2}\rho\ddot{\tilde{\psi}}_2. \quad (2)$$
$$\frac{\partial Q_{13}}{\partial x_1}+\frac{\partial Q_{23}}{\partial x_2}+2\tilde{q}_3=\rho H\ddot{\tilde{r}}$$

where ρ – is the density of the plate material.

Bending, shear moments M_{11}, M_{22}, M_{12} and shear forces Q_{13}, Q_{23} are defined as follows.

$$M_{11}=\int_{-h}^{h}\sigma_{11}zdz=\frac{H^2}{2}\left(E_{11}\frac{\partial\tilde{\psi}_1}{\partial x_1}+E_{12}\frac{\partial\tilde{\psi}_2}{\partial x_2}-E_{13}\frac{2(\tilde{r}-\tilde{W})}{H}\right),$$
$$M_{22}=\int_{-h}^{h}\sigma_{22}zdz=\frac{H^2}{2}\left(E_{12}\frac{\partial\tilde{\psi}_1}{\partial x_1}+E_{22}\frac{\partial\tilde{\psi}_2}{\partial x_2}-E_{23}\frac{2(\tilde{r}-\tilde{W})}{H}\right), \quad (3)$$
$$M_{12}=M_{21}=\int_{-h}^{h}\sigma_{12}zdz=G_{12}\frac{H^2}{2}\left(\frac{\partial\tilde{\psi}_1}{\partial x_2}+\frac{\partial\tilde{\psi}_2}{\partial x_1}\right).$$

$$Q_{13}=\int_{-h}^{h}\sigma_{13}dz=G_{13}\left(2\tilde{u}_1+H\frac{\partial\tilde{r}}{\partial x_1}\right),$$
$$Q_{23}=\int_{-h}^{h}\sigma_{23}dz=G_{23}\left(2\tilde{u}_2+H\frac{\partial\tilde{r}}{\partial x_2}\right). \quad (4)$$

Bimoments P_{11}, P_{22} P_{12}, generated by bending and shear of the plate are determined by the following formulas:

$$P_{11}=\frac{1}{h^2}\int_{-h}^{h}\sigma_{11}z^3dz=\frac{H^2}{2}\left(E_{11}\frac{\partial\tilde{\beta}_1}{\partial x_1}+E_{12}\frac{\partial\tilde{\beta}_2}{\partial x_2}-E_{13}\frac{2(3\tilde{\gamma}-\tilde{W})}{H}\right),$$
$$P_{22}=\frac{1}{h^2}\int_{-h}^{h}\sigma_{22}z^3dz=\frac{H^2}{2}\left(E_{12}\frac{\partial\tilde{\beta}_1}{\partial x_1}+E_{22}\frac{\partial\tilde{\beta}_2}{\partial x_2}-E_{23}\frac{2(3\tilde{\gamma}-\tilde{W})}{H}\right), \quad (5)$$
$$P_{12}=P_{21}=\frac{1}{h^2}\int_{-h}^{h}\sigma_{12}z^3dz=\frac{H^2}{2}G_{12}\left(\frac{\partial\tilde{\beta}_1}{\partial x_2}+\frac{\partial\tilde{\beta}_2}{\partial x_1}\right).$$

Intensities of transverse normal bimoments $\tilde{p}_{13}$, $\tilde{p}_{23}$ and $\tilde{p}_{33}$ are defined by expressions

$$\tilde{p}_{k3} = G_{k3}\left(\frac{2\tilde{u}_k - 4\tilde{\psi}_k}{H} + \frac{\partial \tilde{\gamma}}{\partial x_k}\right), \quad (k = 1,2),$$
$$\tilde{p}_{33} = E_{31}\frac{\partial \tilde{\psi}_1}{\partial x_1} + E_{32}\frac{\partial \tilde{\psi}_2}{\partial x_2} - E_{33}\frac{2(\tilde{r} - \tilde{W})}{H}. \qquad (6)$$

The equations for bimoments in bending and transverse shear are obtained in the following form:

$$\frac{\partial P_{11}}{\partial x_1} + \frac{\partial P_{12}}{\partial x_2} - 3\tilde{p}_{13} + H\tilde{q}_1 = \frac{H^2}{2}\rho\ddot{\tilde{\beta}}_1,$$
$$\frac{\partial P_{21}}{\partial x_1} + \frac{\partial P_{22}}{\partial x_2} - 3\tilde{p}_{23} + H\tilde{q}_2 = \frac{H^2}{2}\rho\ddot{\tilde{\beta}}_2 \quad , \qquad (7)$$
$$H\frac{\partial \tilde{p}_{13}}{\partial x_1} + H\frac{\partial \tilde{p}_{23}}{\partial x_2} - 4\tilde{p}_{33} + 2\tilde{q}_3 = H\rho\ddot{\tilde{\gamma}}.$$

Equations (2) and (7) form a joint system of six equations for nine unknown functions: $\tilde{\psi}_1$, $\tilde{\psi}_2$, $\tilde{\beta}_1$, $\tilde{\beta}_1$, $\tilde{u}_1$, $\tilde{u}_2$, $\tilde{r}$, $\tilde{\gamma}$, $\tilde{W}$.

Equations (2) and (7) contain nine unknown functions, which is insufficient for an unambiguous solution to the problem. Three more equations are required for unambiguity. To construct these missing equations, we expand the displacements u in a Maclaurin series [14]. We present these equations for the problem of bending vibrations:

$$\frac{\partial \tilde{\sigma}_{11}}{\partial x_1} + \frac{\partial \tilde{\sigma}_{12}}{\partial x_2} + \frac{\tilde{\sigma}^*_{13}}{H} = \rho\ddot{\tilde{u}}_1,$$
$$\frac{\partial \tilde{\sigma}_{21}}{\partial x_1} + \frac{\partial \tilde{\sigma}_{22}}{\partial x_2} + \frac{\tilde{\sigma}^*_{23}}{H} = \rho\ddot{\tilde{u}}_2 \quad , \qquad (8)$$

$$\frac{\partial \tilde{q}_1}{\partial x_1} + \frac{\partial \tilde{q}_2}{\partial x_2} + \frac{\tilde{\sigma}^*_{33}}{H} = \rho\ddot{\tilde{W}}. \qquad (9)$$

ISSN 2079-0031 (Print) ISSN 2411-0558 (Online)

Here $\tilde{\sigma}_{11}, \tilde{\sigma}_{12}, \tilde{\sigma}_{22}$ are determined from Hooke's law taking into account the conditions on the front surfaces:

$$\sigma_{11} = E_{11}^{*} \frac{\partial \tilde{u}_1}{\partial x_1} + E_{12}^{*} \frac{\partial \tilde{u}_2}{\partial x_2} + \frac{E_{13}}{E_{33}} \tilde{q}_3,$$
$$\tilde{\sigma}_{22} = E_{12}^{*} \frac{\partial \tilde{u}_1}{\partial x_1} + E_{22}^{*} \frac{\partial \tilde{u}_2}{\partial x_2} + \frac{E_{23}}{E_{33}} \tilde{q}_3, \qquad (10)$$
$$\tilde{\sigma}_{12} = G_{12} \left(\frac{\partial \tilde{u}_1}{\partial x_2} + \frac{\partial \tilde{u}_2}{\partial x_1} \right),$$

$$\frac{\tilde{\sigma}_{3k}^{*}}{H} = G_{k3} \frac{210\left(33\tilde{\beta}_k - 9\tilde{\psi}_k - 4\tilde{u}_k\right)}{H^2}$$
$$+ G_{k3} \frac{\partial}{\partial x_k} \left(\frac{\tilde{q}_3}{E_{33}} - \frac{E_{31}}{E_{33}} \frac{\partial \tilde{u}_1}{\partial x_1} - \frac{E_{31}}{E_{33}} \frac{\partial \tilde{u}_2}{\partial x_2} \right) \qquad (11)$$
$$+ \frac{42}{H} \left(\tilde{q}_k - G_{k3} \frac{\partial \tilde{W}}{\partial x_k} \right), \ (k = 1,2),$$

$$\frac{\tilde{\sigma}_{33}^{*}}{H} = E_{33} \frac{210\left(9\tilde{\gamma} - 2\tilde{W} - \tilde{r}\right)}{H^2}$$
$$+ E_{31} \frac{\partial}{\partial x_1} \left(\frac{\tilde{q}_1}{G_{13}} - \frac{\partial \tilde{W}}{\partial x_1} \right) + E_{32} \frac{\partial}{\partial x_2} \left(\frac{\tilde{q}_2}{G_{23}} - \frac{\partial \tilde{W}}{\partial x_2} \right) \qquad (12)$$
$$+ \frac{30}{H} \left(\tilde{q}_3 - E_{31} \frac{\partial \tilde{u}_1}{\partial x_1} - E_{32} \frac{\partial \tilde{u}_2}{\partial x_2} \right).$$

The system of equations (2), (7) - (9) constitutes a joint system with respect to nine unknown functions $\tilde{\psi}_1$, $\tilde{\psi}_2$, $\tilde{u}_1$, $\tilde{u}_2$, $\tilde{\beta}_1$, $\tilde{\beta}_1$, $\tilde{r}$, $\tilde{\gamma}$, $\tilde{W}$.

Boundary conditions. It is believed that the edges of the plate structure $x_1 = 0,\ x_1 = a,\ x_2 = 0$ and $x_2 = b$ are rigidly fixed. At the fixed edges of the plate structure, the conditions of equality of generalized displacements to zero must be satisfied:

$$\tilde{\psi}_1 = 0,\quad \tilde{\beta}_1 = 0,\quad \tilde{\psi}_2 = 0,\quad \tilde{\beta}_2 = 0,$$
$$\tilde{u}_1 = 0,\ \ \tilde{u}_2 = 0,\ \ \tilde{r} = 0,\ \ \tilde{\gamma} = 0,\ \ \tilde{w} = 0 \ . \qquad (13)$$

Solution method. The methodology and algorithm for numerically solving the problem of vibrations of a plate structure under normal dynamic

ISSN 2079-0031 (Print) ISSN 2411-0558 (Online)

loads are developed using the finite difference method. To approximate the derivatives of displacements with respect to spatial coordinates, we use formulas for central difference schemes. To approximate the derivatives of stresses, forces, moments, and bimoments, we use central finite difference schemes at half-steps, which have second-order accuracy. The conditions for the vanishing force factors of the plate at the free edges are approximated by the vanishing arithmetic mean of the displacements of the external and internal points. The following formulas of the finite difference method are used to approximate the derivatives of displacements, stresses, and force factors.

The derivatives of the functions of generalized displacements at the central point of the partition are determined using the formulas for the central difference.

$$\left(\frac{\partial f}{\partial x_1}\right)_{i,j} = \frac{f_{i+1,j} - f_{i-1,j}}{2\Delta x_1}, \qquad \left(\frac{\partial f}{\partial x_2}\right)_{i,j} = \frac{f_{i,j+1} - f_{i,j-1}}{2\Delta x_2}.$$

When approximating derivatives of stresses, forces, moments and bimoments, central finite-difference schemes on half-steps are used, which have the second order of accuracy:

$$\frac{\partial F_{i,j}^k}{\partial x_1} = \frac{F_{i+\frac{1}{2},j}^k - F_{i-\frac{1}{2},j}^k}{\Delta x_1}, \quad \frac{\partial F_{i,j}^k}{\partial x_2} = \frac{F_{i,j+\frac{1}{2}}^k - F_{i,j-\frac{1}{2}}^k}{\Delta x_2} \quad \left(i = \overline{1,N};\ \ j = \overline{1,M}\right).$$

We represent the second derivative of a function with respect to time within the framework of the finite difference method in the following form:

$$\frac{\partial^2 f_{i,j}^k}{\partial t^2} = \frac{f_{i,j}^{k+1} - 2 f_{i,j}^k + f_{i,j}^{k-1}}{\Delta t^2},$$

where Δt – is the time step.

When implementing the numerical method for solving the given problem, we select the steps in spatial coordinates and time as follows:

$$\Delta x_1 = \frac{a}{N},\ \ \Delta x_2 = \frac{b}{M}, \quad c\Delta t \le \min(\Delta x_1, \Delta x_2).$$

Here $\Delta x_1 = a / N,\ \ \Delta x_2 = b / M$ – is the step in grid method calculation.

ISSN 2079-0031 (Print) ISSN 2411-0558 (Online)

The program for calculating the displacements and force factors of a multi-story building was developed in the Delphi algorithmic environment.

Results analysis. We assume that the plates are made of reinforced concrete with an elastic modulus *E=20,000 MPa*, a density of ρ = *2500 kg/m*^{3}, and a Poisson's ratio of $\nu = 0.3$. The dimensions of the plate structure (thickness, length, and height) are assumed to be *H=1 m, a=10 m, and b=10 m,* respectively. The mesh division numbers are: *N=M=20*.

The normal force $q_3^{(-)}$, is applied to the top of the plate structure in the form of a uniformly distributed force according to the harmonic law.

$$q_3^{(-)} = q_0 \sin(\omega_0 t)\,, \tag{14}$$

where q_0 and ω_0 – the amplitude and frequency of external force. During calculations, the frequency of the external force varies.

Let us introduce dimensionless displacements on the front surfaces of the plate $z = -h$ and $z = +h$ according to the following formulas:

$$\approx{u}_k = \frac{E\tilde{u}_k}{Hq_0}\,,\ \ \approx{\psi}_k = \frac{E\tilde{\psi}_k}{Hq_0}, (k = 1{,}2),\ \ \approx{w} = \frac{E\tilde{w}}{Hq_0},\ \ \approx{r} = \frac{E\tilde{r}}{Hq_0}. \tag{15}$$

We introduce dimensionless stresses using the formulas

$$\approx{\sigma}_{11} = \frac{\tilde{\sigma}_{11}}{q_0},\ \ \approx{\sigma}_{22} = \frac{\tilde{\sigma}_{22}}{q_0}. \tag{16}$$

Figures 2 and 3 show a graph of the change in the generalized longitudinal dimensionless displacement $\approx{\psi}_1$ and generalized transverse dimensionless displacement $\approx{r}$ depending on time *t*, at the frequency of external force $\omega_0 = 100$ rad/s.

ISSN 2079-0031 (Print) ISSN 2411-0558 (Online)

$\tilde{\tilde{\psi}}_1$

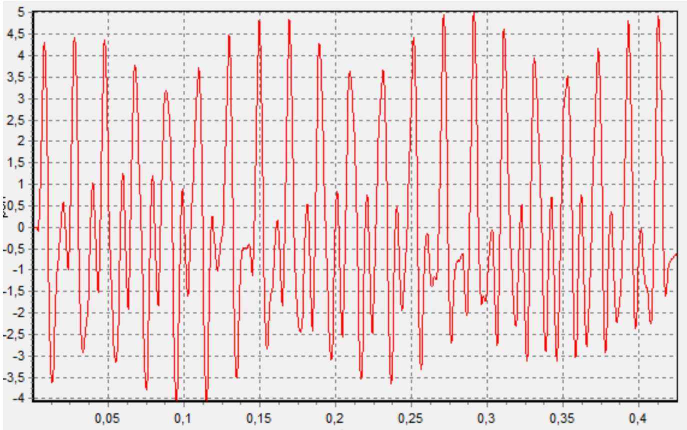

t (s)

Figure 2. Graph of changes in the generalized longitudinal dimensionless displacement $\tilde{\tilde{\psi}}_1$ depending on time *t*, at the frequency of external force $\omega_0 = 100$ rad/s.

$\tilde{\tilde{r}}$

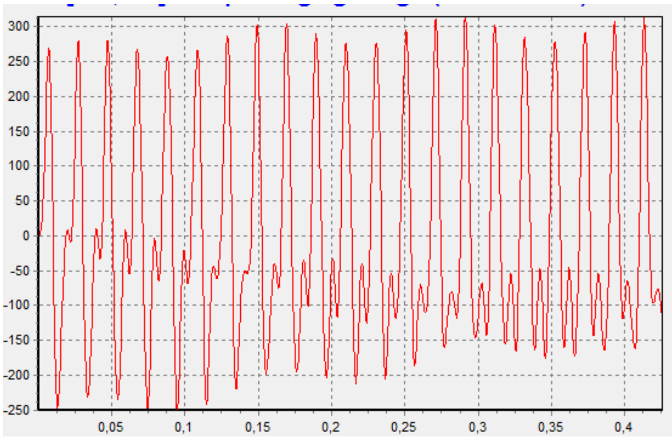

t (s)

Figure 2. Graph of changes in the generalized transverse dimensionless displacement $\tilde{\tilde{r}}$ depending on time *t*, at the frequency of external force $\omega_0 = 100$ rad/s.

Figure 4 shows the oscillation modes in the generalized longitudinal dimensionless displacement $\tilde{\tilde{\psi}}_1$ in the generalized transverse dimensionless displacement $\tilde{\tilde{r}}$ at the frequency of external force $\omega_0 = 100$ rad/s.

ISSN 2079-0031 (Print) ISSN 2411-0558 (Online)

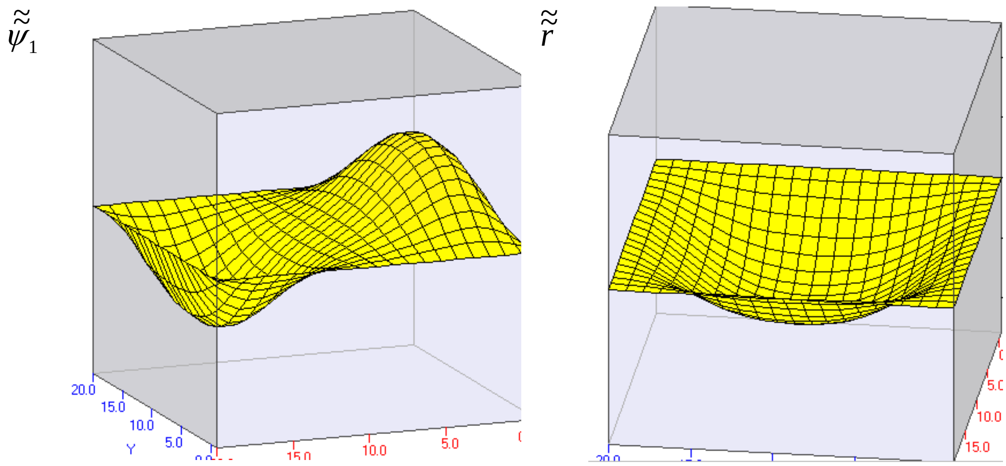

(a) *(b)*

Figure 4.The oscillation modes in the generalized longitudinal dimensionless displacement $\tilde{\tilde{\psi}}_1$ in the generalized transverse dimensionless displacement $\tilde{\tilde{r}}$ at the frequency of external force $\omega_0 = 100$ rad/s.

Figures 5 and 6 show the changes in the generalized longitudinal dimensionless displacement $\tilde{\tilde{\psi}}_1$ and generalized transverse dimensionless displacement $\tilde{\tilde{r}}$ plotted near the eigenfrequency, i.e., when the plate state transitions to the resonant mode.

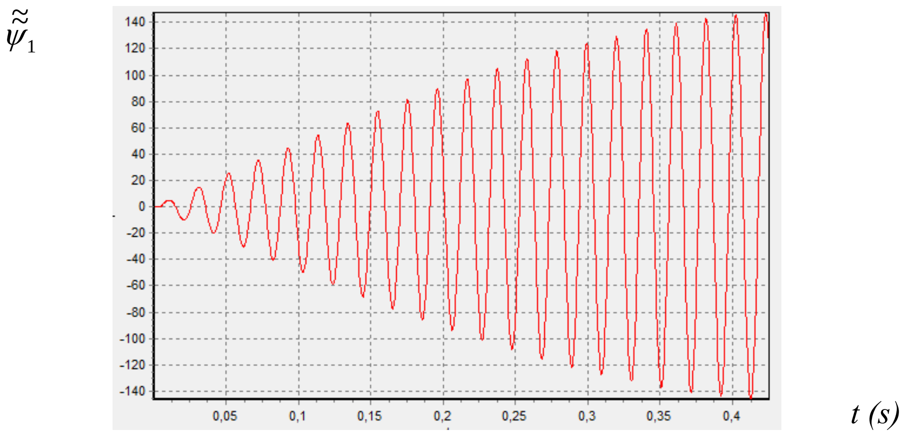

Figure 5. Graph of changes in generalized longitudinal dimensionless displacement depending on time *t*, at the frequency of external force $\omega_0 = 50$ rad/s.

ISSN 2079-0031 (Print) ISSN 2411-0558 (Online)

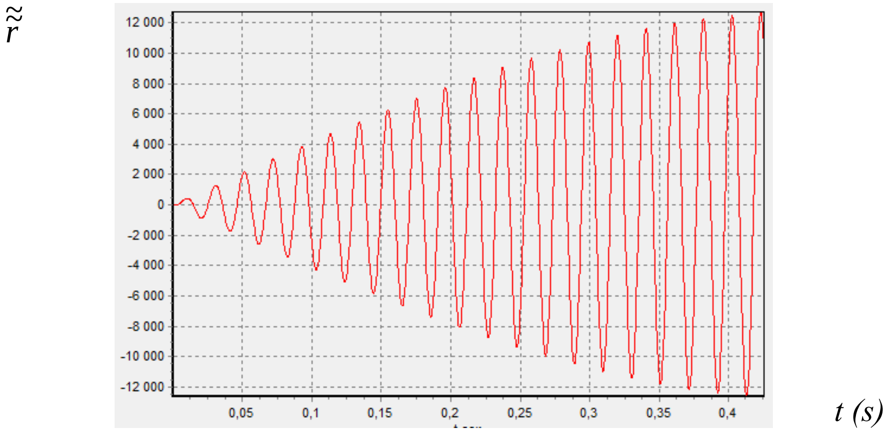

Figure 6. Graph of change in generalized transverse dimensionless displacement $\tilde{\tilde{r}}$ depending on time *t*, at the frequency of external force $\omega_0 = 50$ rad/s.

Figure 4 shows the oscillation modes in the generalized longitudinal dimensionless displacement $\tilde{\tilde{\psi}}_1$ in the generalized transverse dimensionless displacement $\tilde{\tilde{r}}$ at the frequency of external force $\omega_0 = 50$ rad/s.

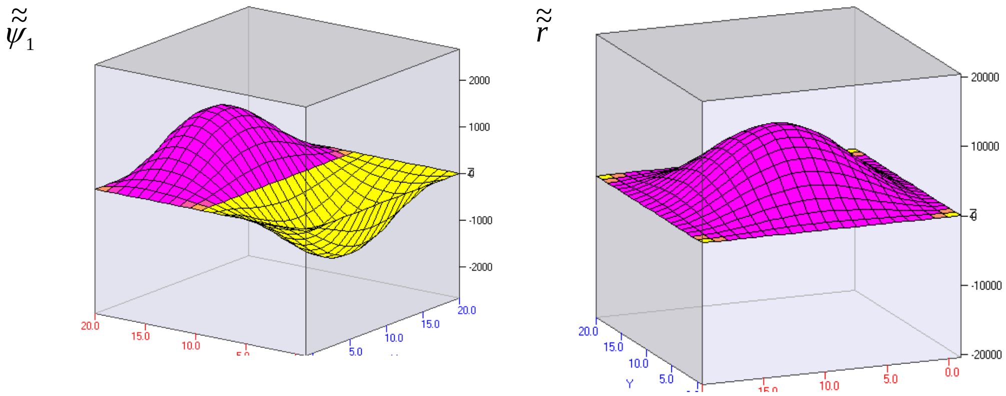

(a) *(b)*

Figure 4. The oscillation modes in the generalized longitudinal dimensionless displacement $\tilde{\tilde{\psi}}_1$ in the generalized transverse dimensionless displacement $\tilde{\tilde{r}}$ at the frequency of external force $\omega_0 = 50$ rad/s.

ISSN 2079-0031 (Print) ISSN 2411-0558 (Online)

Table 1 shows the maximum values of displacement of a plate structure at different frequencies of external force ω_0 .

Table 1.

Maximum displacement values, at midpoint $(x_1 = a/11,\ x_2 = b/11)$ of plate structure at different frequencies of external force ω_0 .

ω_0 , $\left(in\ \frac{rad}{s}\right)$	(x_1, x_2)	$\frac{E\,\tilde{r}}{Hq_0}$	$\frac{E\,\tilde{w}}{Hq_0}$	$\frac{E\,\tilde{u}_1}{Hq_0}$	$\frac{E\,\tilde{u}_2}{Hq_0}$	$\frac{E\,\tilde{\psi}_1}{Hq_0}$	$\frac{E\,\tilde{\psi}_2}{Hq_0}$
100	$\left(x_1 = \frac{a}{11}, x_2 = \frac{b}{11}\right)$	311,360	308,08	14,922	14,922	4,956	4,956
70		634,149	642,790	25,634	25,634	8,285	8,285
50 **(resonant state)**		**12717,051**	**12596,383**	**449,647**	**449,647**	**147,565**	**147,565**
30		731,442	727,923	25,069	25,091	8,112	8,113

Above, we calculated the numerical values of the generalized displacements of the plate at resonance and near-resonance states using the mathematical model we constructed for the plate and the program we wrote for it. Now let us examine the stress state of the plate at resonance and near-resonance states.

Figures 8 and 9 show graphs $\tilde{\sigma}_{11}/q_0$ and $\tilde{\sigma}_{22}/q_0$ at the values of the frequency of external force.

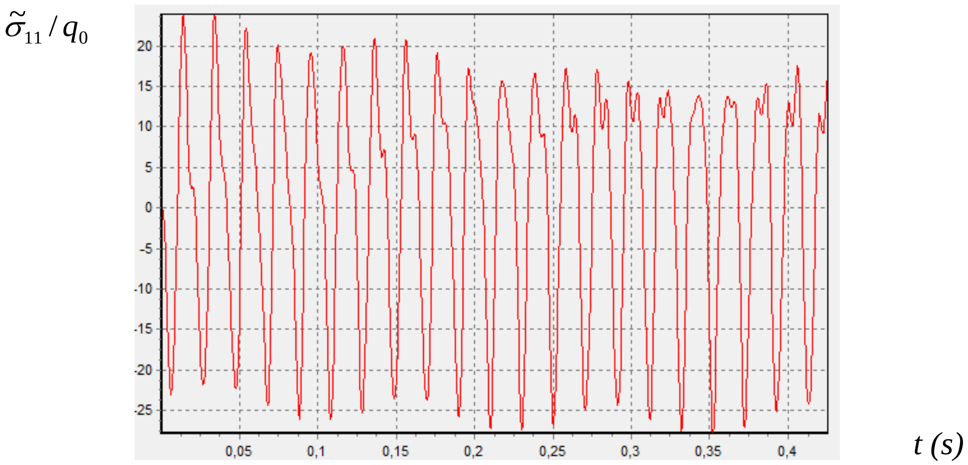

Figure 8. Graph $\tilde{\sigma}_{11}/q_0$, at the frequency of external force $\omega_0 = 100$ rad/s.

ISSN 2079-0031 (Print) ISSN 2411-0558 (Online)

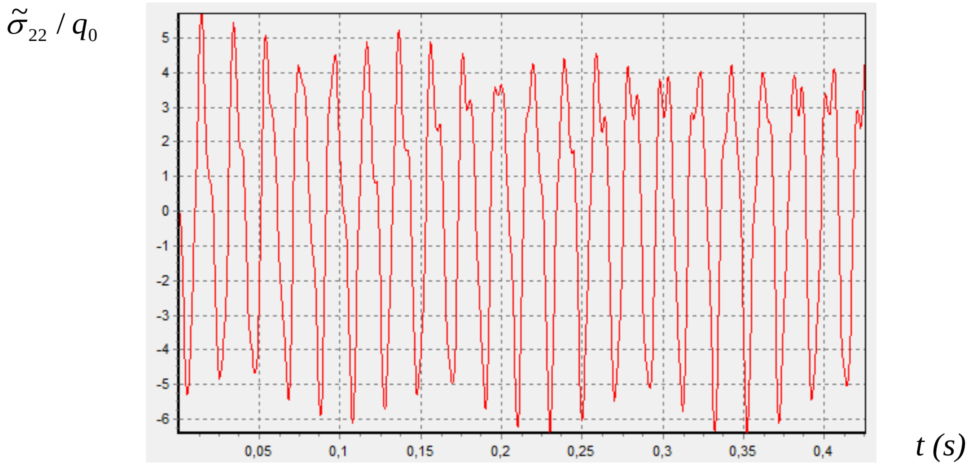

Figure 9. Graph $\tilde{\sigma}_{22} / q_0$, at the frequency of external force $\omega_0 = 100$ rad/s.

Figures 10 and 11 show the graphs $\tilde{\sigma}_{11} / q_0$ and $\tilde{\sigma}_{22} / q_0$ plotted near the eigenfrequency, i.e., when the plate state transitions to the resonant mode.

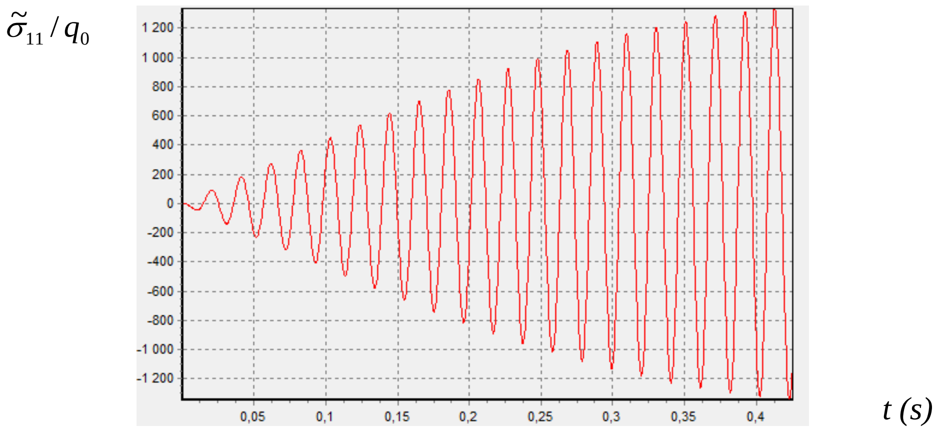

Figure 10. Graph of change in $\tilde{\sigma}_{11} / q_0$ at the frequency of external force $\omega_0 = 50$ rad/s.

ISSN 2079-0031 (Print) ISSN 2411-0558 (Online)

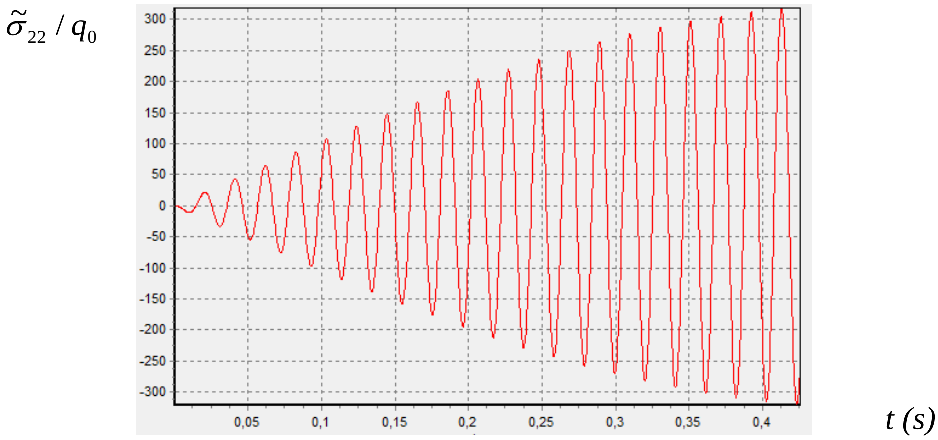

Figure 11. Graph of change in $\tilde{\sigma}_{22} / q_0$ at the frequency of external force $\omega_0 = 50$ rad/s

Figure 12 shows the oscillation modes $\tilde{\sigma}_{11} / q_0$ in coordinates x_1, x_2 and z, at the values of the frequency of external force $\omega_0 = 100$ rad/s and $\omega_0 = 50$ rad/s.

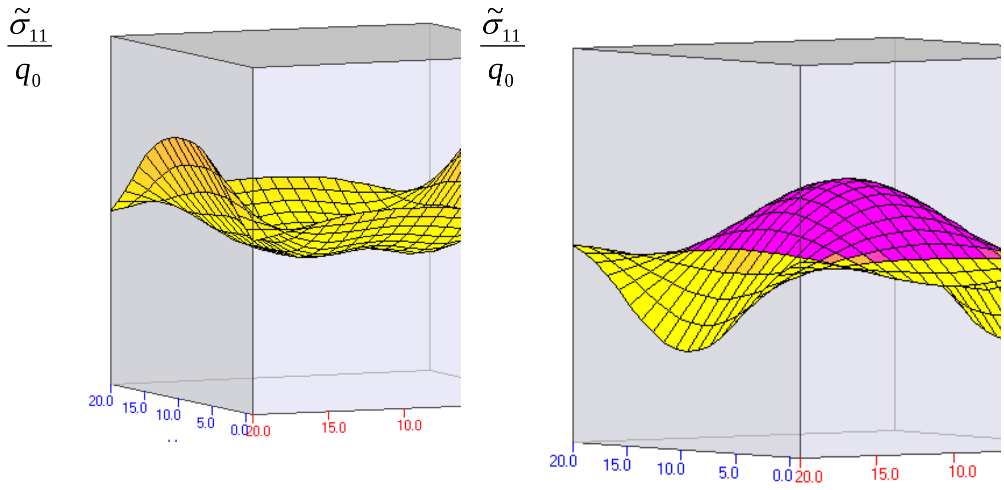

$\omega_0 = 100$ rad/s. $\omega_0 = 50$ rad/s.

Figure 12. Oscillation modes $\tilde{\sigma}_{11} / q_0$ in coordinates x_1, x_2 and z, at the values of the frequency of external force $\omega_0 = 100$ rad/s and $\omega_0 = 50$ rad/s.

ISSN 2079-0031 (Print) ISSN 2411-0558 (Online)

Table 2 shows the ratio of normal stress values $\tilde{\sigma}_{11}/q_0$ and $\tilde{\sigma}_{22}/q_0$ to the value of the amplitude of external force q_0 for different frequencies of external force ω_0. When studying the stress state of the plate by calculating using the program, it was found that the maximum values $\tilde{\sigma}_{22}/q_0$ are achieved at the plate point $(x_1 = a/20,\ x_2 = b/11)$ and maximum values $\tilde{\sigma}_{22}/q_0$ are achieved at the plate point $(x_1 = a/11,\ x_2 = b/20)$, respectively. Therefore, Table 2 presents the stress values recorded at these points.

Table 2.

Values of normal stresses σ_{11}/q_0 and σ_{22}/q_0, and the value of external force q_0 for different values of natural oscillations ω_0.

ω_0, $(in\ \ rad/s)$	$(x_1,\ x_2)$	$\tilde{\sigma}_{22}/q_0$.	$\tilde{\sigma}_{22}/q_0$
100	$(x_1 = a/20,\ x_2 = b/11)$	26,447	26,447
	$(x_1 = a/11,\ x_2 = b/20)$	6,391	6,391
70	$(x_1 = a/20,\ x_2 = b/11)$	64,948	64,948
	$(x_1 = a/11,\ x_2 = b/20)$	15,197	15,197
50 **(resonant state)**	$(x_1 = a/20,\ x_2 = b/11)$	**1245,930**	**321,221**
	$(x_1 = a/11,\ x_2 = b/20)$	**321,221**	**1245,930**
30	$(x_1 = a/20,\ x_2 = b/11)$	80,072	80,072
	$(x_1 = a/11,\ x_2 = b/20)$	18,912	18,912

Symmetry of stress values $\tilde{\sigma}_{11}/q_0$ and $\tilde{\sigma}_{22}/q_0$ can be explained by the fact that the plate has a square shape. Consequently, even refined theories that do not consider transverse compressibility of the plate material are not suitable for dynamic calculations of the plate near the resonant mode.

Conclusion.

Based on the conducted research, the following conclusions are drawn:

A spatial bimoment theory is proposed that is suitable for describing the dynamic behavior of plates under forced vibrations.

The proposed bimoment theory of plates enables dynamic calculations of anisotropic thick plates taking into account the spatial stress-strain state. Accurate formulas are constructed for determining the internal forces, moments, bimoments, and generalized displacements of plates. These formulas enable the determination of the maximum values of generalized displacements and stresses of plates.

Dynamic calculation methods are developed for determining the displacements, internal forces, moments and bimoments of plates under various edge fixation and external loading options.

A method for dynamic calculations of thick plates under external periodic loading is developed. This method enables the evaluation of the dynamic behavior of thick plates near the resonant state.

A spatial dynamic plate model is developed within the framework of bimoment theory that is suitable for describing the dynamic behavior of buildings under seismic vibrations.

References

1. Benerjee S, Kundu T 2006 Journal of Acoustical Society of America 119(4) 2006-2017.

2. Kh. Kh. Khudoynazarov, R.I. Khalmuradov, B.F. Yalgashev, "Longitudinal-radial vibrations of a elastic cylindrical shell filled with a viscous compressible liquid", Bulletin of Tomsk State Univ. Math. Mekh., 2021, no. 69, 139–154.

3. Safarov, I.I., Teshayev, M.K., Boltayev, Z.I. and Akhmedov, M.S, International Journal of Theoretical and Applied Mathematics, 3, pp. 191-198 (2017).

4. Xiang S, Jin Ya, Bi Z, Jiang Sh, Yang M 2011 Composite Structures 93(11) 2826-2832.

5. C.E. İmrak and İ. Gerdemeli. An Exact Solution for the Deflection of a Clamped Rectangular Plate under Uniform Load // Journal of Applied Mathematical Sciences, Vol. 1, 2007, no. 43, 2129 – 2137., https://www.researchgate.net/publication/267078798

6. I.A. Wojtaszak, The calculation of maximum deflection, moments, and shear for uniformly loaded rectangular plate with clamped edge, J. Appl. Mechanics, Trans. ASME, 4 (1937), A173-A176.

7. S.P. Timoshenko and S. Woinowsky-Krieger, Theory of Plates and Shells (2nd edn.), McGraw-Hill, New York, 1959.

8. C.E. İmrak and I. Gerdemeli, A numerical method for clamped thin rectangular plates carrying a uniformly distributed load, Int. J. Appl. Mech. No.3 (2007).

9. C.E.Imrak and I. Gerdemeli, The problem of isotropic rectangular plate with four clamped edges, Indian Academy of Sciences SADHANA (2007).

10. Singal R. K., Gorman D. J., Forques S. A., A comprehensive analytical solution for free vibration of rectangular plates with classical edge conditions: Experimental verification, Exp. Mech. 32 (1) (1992) 21–23.

11. N.Kh. Mirzakabilov, Methods for calculating vibrations of a viscoelastic multilayer (three-layer) plate // Universum: technical sciences: electronic scientific journal 2024. 7(124). https://7universum.com/ru/tech/archive/item/18008

12. Xiang Liu, Yu Li, Yuliang Lin, J.R. Banerjee, Spectral dynamic stiffness theory for free vibration analysis of plate structures stiffened by beams with arbitrary cross-sections // Thin-Walled Structures 160 (2021) 107391, https://doi.org/10.1016/j.tws.2020.107391

13. M. Usarov, A. Salokhiddinov, D. Usarov, I. Khazratkulov and N. Dremova, "To the theory of bending and oscillations of three-layered plates with a compressible filler" in *International Conference Reliability of buildings and constructions - 2020*, IOP Conference 896, edited by D. Nazarov (IOP Publishing, Tashkent, 2020), 052037.

14. M. Mirsaidov, M. Usarov, "Bimoment theory construction to assess the stress state of thick orthotropic plates" in *International Scientific Conference "Earth and Environmental Science" – 2020,* E3S Web of Conferences, 971, edited D. Nazarov, (EDP Sciences, Tashkent, 2020), 032041.

15. M. Usarov and F. Usanov, "On solution of the problem of bending and vibrations of thick plates on the basis of the bimoment theory" in *International Conference on Actual Problems of Applied Mechanics-2021*, AIP Conference Proceedings 2637, edited by F. Tangreti (AIP Publishing, Samarkand, 2022), 0118598.

16. M. Usarov, D. Usarov and G. Mamatisaev, "Calculation of a Spatial Model of a Box-Type Structure in the LIRA Design System Using the Finite Difference Method," in *XV International Online Conference Improving Farming Productivity And Agroecology–Ecosystem Restoration–2023,* E3S Web of Conferences 403, edited by R. Bennacer (EDP Sciences, Tashkent, 2023), pp.1267–1275.

17. M. Usarov, G. Mamatisaev, J. Yarashov, and E. Toshmatov, "Non-stationary oscillations of a box-like structure of a building" in *Modelling and Methods of Structural Analysis – 2019,* IOP Conference 1425, edited by A. Volkov *et al*. (IOP Publishing, Moscow, 2019), 012003.

Надійшла (received) 05.01.2026
Стаття прийнята до друку 25.01.2026
Опублікована 27.03.2026

Makhmatali Usarov, Dr. Phys.-Math. Sci, Professor
Institute of Mechanics and Seismic Stability of Structures named after M.T.Urazbaev, Uzbekistan Academy of Sciences,
Str. Durmon yuli 40, Tashkent, Uzbekistan, 100125,
Тел: -998 (90) 374-38-78. E-mail: umakhamatali@mail.ru
ORCID ID: 0000-0001-7848-3696

ISSN 2079-0031 (Print) ISSN 2411-0558 (Online)

Shuhrat Askarhodjaev senior researcher,
Institute of Mechanics and Seismic Stability of Structures named after M.T.Urazbaev,
Uzbekistan Academy of Sciences,
Str. Durmon yuli 40, Tashkent, Uzbekistan, 100125,
Тел: +998 (90) 130-30-90. E-mail: shuhrat1608@gmail.com
ORCID ID: 0000-0001-5367-4541

Furqat Usanov, junior researcher,
Institute of Mechanics and Seismic Stability of Structures named after M.T.Urazbaev,
Uzbekistan Academy of Sciences,
Str. Durmon yuli 10, Tashkent, Uzbekistan, 100125,
Тел: +998 (90) 032-94-01. E-mail: usanovfurqat94@mail.ru
ORCID ID: 0000-0002-3475-9272

УДК 539.3

Поперечні коливання пластинчастої конструкції з закріпленими всіма сторонами під нормальними навантаженнями / Махматалі Усаров, Шухрат Аскарходжаєв, Фуркат Усанов // Вісник НТУ "ХПІ". Серія: Інформатика та моделювання. – Харків: НТУ "ХПІ". – 2026. – № 2 (16). – С. 59 – 79.

У цій статті розглядаються поперечні коливання прямокутної пластинчастої конструкції, всі сторони якої закріплені, під дією нормальних навантажень, прикладених до її поверхні, з використанням теорії бімоментних пластин. Задачу було вирішено методом скінченних різниць. Представлено числові результати розрахунку нормальних переміщень та напружень. Іл.: 2. Табл.: 5. Бібліогр.: 10 назв

Ключові слова: переміщення, напруження, моменти, бімоменти, теорія бімоментів, нормальне навантаження, зсувне навантаження, рівняння руху, граничні умови, метод скінченних різниць.

UDK 539.3

Transverse oscillation of a plate structure with all sides fixed under normal loads / Makhmatali Usarov, Shukhrat Askarkhodjaev, Furqat Usanov // Herald of the National Technical University "KhPI". Series of "Informatics and Modeling". –Kharkov: NTU "KhPI". – 2026. – No 2 (16). – P. 59–79.

This article examines the transverse vibration of a rectangular plate structure, with all sides fixed, under normal loads applied to its surface using bimoment plate theory. The problem was solved using the finite difference method. Numerical results for calculating the normal displacements and stresses are presented. Fig.: 2. Tables: 5. References: 10.

Keywords: displacements, stresses, moments, bimoments, bimoment theory, normal load, shear load, equations of motion, boundary conditions, finite difference method.